The International Journal of Life Cycle Assessment
https://doi.org/10.1007/s11367-025-02454-7

BUILDING COMPONENTS AND BUILDINGS

Integrating life cycle assessment (LCA) and machine learning for sustainable designs: a case study on protective layers made of mineral-bonded fiber-reinforced composites

Isabela de Paula Salgado[1,2] · Felix Conrad[3] · Cesare Signorini[2] · Edeltraud Günther[1,4] · Steffen Ihlenfeldt[3] · Viktor Mechtcherine[2]

Received: 15 October 2024 / Accepted: 14 March 2025

Abstract

Purpose In recent years, machine learning (ML) has become an important tool for predicting material properties and optimizing their mechanical performance without the need for large data sets. However, when design considerations only target structural characteristics, sustainability issues are often overlooked, leading to increased carbon dioxide emissions, energy consumption, and over-reliance on non-renewable materials. This study seeks to bridge this gap by optimizing the design of impact-resistant fiber-reinforced cement-based composites through a sustainability-driven, ML-based modeling approach.

Methods In this context, we propose a three-stage integrated framework that combines experimental test databases, sustainability assessment, and ML modeling. The specific design scenario considered here is the use of these materials as protective layers for concrete structures under impact loading. A variety of combinations of fiber and/or textile-reinforced cementitious composites were considered, including single and multiple layers. A life cycle assessment (LCA) was performed in terms of global warming potential (GWP), as this is a sensitive and critical environmental parameter in the concrete industry. The experimental data, consisting of 193 tests on composites subjected to hard impacts, measured the dissipated energy and ballistic limits. Principal component analysis (PCA) was employed to identify patterns and correlations within the experimental data. Based on the database, an ML model was developed to predict energy dissipation, enabling optimization for untested configurations. A multi-objective optimization (MOO) strategy was applied to balance the energy dissipation and GWP constraints, enabling the identification of Pareto-optimal solutions that represent the best trade-offs between mechanical performance and environmental impact.

Conclusions The ML model demonstrated high accuracy in predicting GWP and energy dissipation, closely matching experimental data for tested configurations and indicating strong generalization potential for unseen cases. For severe impact applications (above 4 kJ of impact energy), carbon textile grids outperformed other reinforcements, achieving a 20% performance increase with two layers of textile, while maintaining emissions at 5–6 kg CO_2 equivalent per plate. Glass emerged as the best alternative for strict GWP limits. Remarkably, hybrid composites, despite their higher cement content in comparison to conventional textile-reinforced concrete (TRC), are the most viable choice due to the superior toughness attained due to short fibers and the sustainability benefits of limestone calcined clay cement (LC^3) blended binders. Ultimately, the ML model and LCA framework developed in this study can be extended to other material systems and design scenarios.

Keywords Life cycle assessment · Machine learning · Optimization · Fiber-reinforced composites · Textile-reinforced concrete · Strain-hardening cementitious composites · Limestone calcined clay cement

1 Introduction

Following the pandemic and the subsequent economic recovery, the construction sector experienced significant growth, driven by increased demand for residential, commercial, and infrastructure purposes (IPCC 2023). As these projects resumed, the resource demand and energy consumption for sourcing and transportation increased sharply (IPCC 2023; Ebekozien et al. 2023). This trend of material exploitation is consistent with the projections by the Organization for Economic Cooperation and Development (OECD) that global

Communicated by Daniela Sica.

Extended author information available on the last page of the article

Published online: 09 April 2025

raw material use will nearly double by 2060, with construction materials being the largest contributor (OECD 2019).

Moreover, material consumption and resource depletion are not the only environmental concerns associated with the construction industry. In fact, buildings are responsible for 37% of global energy-related carbon dioxide (CO_2) emissions, while concrete contributes 8% of anthropogenic greenhouse gas (GHG) emissions (United Nations Environment Programme 2024; Miller et al. 2016), largely due to the production of cement clinker, which is the primary binding phase in cement and requires heating limestone and other raw materials above 1400°C in energy-intensive kilns (Chaudhury et al. 2023). This process not only consumes vast amounts of fossil fuels but also releases significant CO_2 from limestone decomposition, making clinker production the dominant source of the emissions related to cement.

Alternative materials and technologies, such as partial cement replacement and incorporation of supplementary cementitious materials (SCMs), are viable solutions (Tushar et al. 2022; Li et al. 2019; Reddy et al. 2021; Donnini et al. 2024). Among these, limestone calcined clay cement (LC^3) has gained attention as a promising low-carbon alternative, capable of reducing clinker content even beyond 50% while maintaining comparable mechanical performance and durability (Scrivener et al. 2018; Schneider et al. 2011; Ahmed et al. 2024).

However, material optimization alone is insufficient. Without the implementation of sustainable design practices and an understanding of the intricate connections between resource consumption, waste generation, and climate consequences—referred to here as the *material-climate-waste nexus*—inevitable and pressing risks to public health and ecosystems will persist (Imbabi et al. 2012; Belaïd 2022; Bleischwitz et al. 2018). In this direction, it is imperative the development and implementation of integrated design approaches, which take into account, on the one hand, the fulfillment of the required structural standards and, on the other hand, the optimization of material consumption and the minimization of the corresponding environmental impact.

Among the existing methodologies to accurately assess the individual contributions of construction materials to the overall life cycle of the system, life cycle assessment (LCA) stands out as a comprehensive, iterative, multi-parametric assessment tool for the environmental component of sustainability. LCA methodology was standardized in the ISO 14040 and 14044 series (International Organization for Standardization 2006a, b). A key part of the process is the creation of a life cycle inventory (LCI), which details all the inputs and outputs of the system over its lifetime. Based on the LCI data, the life cycle impact assessment (LCIA) quantifies the environmental impact of the system by considering a number of categories, including global warming potential (GWP), energy consumption, and resource use. Results are weighted and normalized for comparison.

Nevertheless, the complexity of LCA often leads to misinterpretation and poses challenges in comparing its results without a thorough understanding of the underlying data (Panesar et al. 2017; Scope et al. 2021). These issues are often related to incomplete and inconsistent data, either due to gaps in the product life cycle, limited information on recycled materials and emerging technologies, or uncertainties in long-term scenarios (Ghoroghi et al. 2022). A review of LCA studies (Aggarwal et al. 2024) highlights similar issues, where variations in methodological assumptions lead to discrepancies in GWP estimates, even for similar material systems, further complicating the standardization and comparability of results.

Moreover, the application of LCA to complex systems often demands extensive and detailed data, which can be difficult to obtain. For instance, assessing the environmental impact of a typical reinforced concrete (RC) building requires comprehensive information on product flows, transportation, on-site activities, and material processing. The process remains largely manual, demanding recalculations for each case (D'Amico et al. 2019b). For fiber-reinforced cementitious composites, these challenges are amplified by the variability in mix compositions, reinforcement types, and processing techniques, further complicating impact assessments. Furthermore, conventional LCA methods rely heavily on static datasets, making them less adaptable to real-time design changes and dynamic material performance evaluations.

Machine learning (ML) offers a variety of promising approaches to fill this gap. Indeed, patterns in existing data sets can be identified and processed to develop algorithms that can predict missing data, estimate impact assessment outcomes, and improve scenario analysis (D'Amico et al. 2019b; Ghoroghi et al. 2022). The accuracy of the model can then be enhanced through optimization techniques and AI-driven uncertainty quantification, improving the performance of the system throughout its life cycle.

ML approaches are increasingly being integrated into LCA frameworks to enhance sustainability assessments, optimize impact quantification, and improve decision-making in civil engineering applications (Romeiko et al. 2023; Anand and Amor 2017; Bueno et al. 2016). Ghoroghi et al. (2022), for instance, reviewed ML applications in LCA and found that ML models can reduce uncertainty by predicting environmental impacts based on dynamic datasets. These models integrate large-scale environmental data, material-specific parameters, and life cycle variations, offering a more adaptable approach than traditional LCA. Similarly, Martínez-Ramón et al. (2024) proposed three ML-based frameworks to improve the accuracy and efficiency of LCA calculations

by estimating missing LCI data, replacing resource-intensive simulations, and evaluating impacts based on system parameters. By applying artificial neural networks (ANNs) and decision tree models, they enhance consistency in impact assessments, particularly for GWP and energy consumption.

Duprez et al. (2019) investigated the prediction of life cycle impacts by using three metamodels to estimate the GWP of a building, incorporating new design alternatives. The study results emphasized the effectiveness of ANNs, which were also relied upon by D'Amico et al. (2019a) for a detailed energy and environmental assessment of a building, with the adoption of six environmental indicators. Sharif and Hammad (2019) created an efficient ANN model that calculates the optimal rehabilitation scenario for a building based on total energy consumption, life cycle costing (LCC), and LCA for multiple alternatives. Similarly, Azari et al. (2016) used a hybrid ANN and genetic algorithm-based technique to determine the best possible design combination in terms of energy consumption and life cycle contribution to several environmental impact categories.

Beyond impact assessment, ML has been instrumental in materials optimization, where its ability to analyze complex, multi-variable interactions has led to more efficient mix design formulations and improvements in sustainability. Several studies have explored multi-criteria optimization in materials design, particularly in the optimization of concrete mix designs with a focus on both mechanical performance and sustainability (Sun et al. 2023; Zhang et al. 2020a, 2021). In general, solving multiobjective material design optimization problems leads to a large number of optimal solutions because the ideal design parameters for different properties are often in conflict. These solutions, known as "Pareto-optimal" solutions, reflect trade-offs where the improvement of one property inevitably leads to the compromise of another. Shahrokhishahraki et al. (2024) developed an ML model to optimize cement content in sustainable concrete, reducing emissions while maintaining mechanical performance. Similarly, Asadi Shamsabadi et al. (2023) applied ML-based genetic optimization algorithms to refine multi-objective concrete mix designs, integrating sustainability metrics such as GWP. According to the classification proposed by Hanaoka (2021), optimization approaches can be distinguished into "*few solution inverse designs*" and "*many solution inverse designs*." As a key example of the former approach to construction materials, Naseri et al. (2020) used scalarization with a weighted sum of objectives to transform the multi-objective task into a single-objective task, in order to optimize cost, sustainability (measured in terms of CO_2 emissions and energy consumption), and compressive strength. Sun et al. (2023) incorporated the analytic hierarchy process (AHP) to determine the weights of the optimization objectives and set up two distinct use cases: minimizing the costs and CO_2 emissions. They extended the scope of optimization by considering compressive strength, flexural strength, and processing properties like fluidity and shrinkage.

In the framework of the latter class of approaches, Zhang et al. determined a Pareto front and chose from this the best design with the technique for order preference by similarity to an ideal solution (TOPSIS) for the optimization of the compressive strength for different kinds of concrete mixtures. In their studies, the research group used several additional optimization objectives and different optimization algorithms to determine the Pareto front. They additionally optimized the costs and used multi-objective particle swarm optimization (MOPSO) (Zhang et al. 2020b), costs plus emitted CO_2 determined based on cement content, with the multi-objective firefly algorithm (MOFA) (Zhang et al. 2020a) and the multi-objective bat algorithm (MOBAS) (Zhang et al. 2021).

Huang et al. (2020) optimized the concrete mix of steel fiber-reinforced concrete, in terms of compressive strength, tensile or flexural strength, and cost. They determined the Pareto front and used an efficiency ratio using the difference in cost divided by the difference in strength to obtain the best design. Another strategy combines the "*find goal design*" and "*inverse designs with many solutions*" approaches. By setting constraints on all but one optimization objective and optimizing the remaining objective, the Pareto front can be determined in a step-wise fashion. Asadi Shamsabadi et al. (2023) used this approach for the parallel optimization of two objectives out of cost, GWP, acidification potential (AP), and fossil fuel depletion potential (FDP) for a given composite strength using a genetic optimization algorithm. Naseri et al. (2022) optimized the concrete mixture for four concrete strength classes to minimize a developed environmental index based on the weighted sum of GWP, disposal of hazardous waste, non-hazardous waste, and radioactive waste generated during the production of 1 m^3 concrete.

Collectively, these studies demonstrate the diverse methodologies and considerations in optimizing materials and structural designs, emphasizing the integration of ML models for efficient multi-objective optimization of performance and sustainability metrics, thus serving as robust benchmarks for our analysis.

Focus and significance of the research

This study outlines the concept of a combined multi-criteria design approach to optimize the design of fiber-reinforced cement-based composites in civil engineering applications. The approach integrates mechanical and sustainability considerations by incorporating LCA into an advanced ML scheme (Conrad et al. 2024). A specific case study is presented and discussed to determine the ideal design of protective fiber- and textile-reinforced composites to maximize the energy dissipation capacity as the main mechanical

performance parameter, while minimizing the environmental impact as assessed by LCA.

The primary research objective of this study is to develop an integrated ML-based multi-objective optimization framework that identifies the most efficient fiber-reinforced cementitious composite designs for impact protection. This is achieved by coupling experimental impact test data with sustainability constraints derived from LCA, enabling the selection of configurations that maximize energy dissipation while minimizing GWP. The developed methodology can be extended to other cementitious composite applications where trade-offs between performance and sustainability are critical.

This case study is of particular interest because, in structural protection, the compelling need for high levels of robustness, safety, and resilience often diverges from sustainability concepts (Derissen et al. 2011; Anwar et al. 2020; de Paula Salgado et al. 2025). In particular, fiber- and textile-reinforced composites, namely textile-reinforced concrete (TRC) and strain-hardening cement-based composites (SHCC), while ensuring significant energy dissipation as documented in many studies (Ding et al. 2022; Qin et al. 2020; Tawfik et al. 2023), face some challenges, such as the high binder requirement due to the absence of coarse aggregates in the mix compared to conventional concrete, which raises concerns in terms of emissions and high cost of raw constituents (He et al. 2023). On the other hand, the efficiency of SHCC and TRC allows for reduced material use without compromising load-bearing capacity and toughness, leading to longer service life and reduced maintenance requirements, ultimately providing environmental benefits (Zea Escamilla and Wallbaum 2011). In addition, recent research has focused on exploring pathways towards more sustainable fiber-reinforced composites through the use of more viable matrices and lower grade fibers (Signorini and Nobili 2022), without impairing strain capacity and toughness (Ahmed et al. 2024).

The current case study considers and builds on a database of impact tests on a variety of SHCC, TRC, and TR-SHCC (hybrid) composite plates (Hering et al. 2021, 2023; Signorini et al. 2023) by means of an integrated approach including a sustainability indicator (namely the GWP) in a ML-assisted optimization.

Section 2 presents the concept of the integrated design, starting from the data sets used for the analysis (Section 2.1). Then, the description of the integrated model is presented, detailing the LCA approach adopted here to evaluate the sustainability performance of the protective composites (Section 2.2), including the boundaries and the limitations, and the ML model in which LCA was integrated for defining optimized designs (Section 2.3). Exemplary results for optimized designs obtained in three different scenarios of impact protection are presented and discussed, with mild, medium, and severe input impact energy to be dissipated (Section 3).

2 Methodology

2.1 Experimental data sets: impact testing

The experimental data sets considered in this study refer to previous investigations on the practical assessment of the mechanical behavior of different mineral-bonded composites subjected to hard impact (Hering et al. 2021; Signorini et al. 2023). The tests were performed in an accelerated drop tower developed by Kühn and Curbach (2015) on composite plates with dimensions of $61 \times 61 \times 3\,\mathrm{cm}^3$, which are clamped at the edges by a steel frame. The plates are struck by a rigid cylindrical impactor with a diameter of 10 cm, a mass of 8.4 kg, and a rounded tip, propelled by compressed air from a distance of approximately 11 m. The input impact energy is predetermined by adjusting the pressure of the compressed air and is accurately calculated by measuring the impactor velocity prior to collision. In the case of rebound or perforation, the residual velocity of the projectile (and, therefore, its residual kinetic energy) is measured after the impact occurs. The change in kinetic energy indicates the extent of energy absorbed by the composite plate.

Tests on the same material combination were performed considering a wide spectrum of input energy in order to estimate its ballistic limit—E_{bl}, defined as the minimum impact energy (and thus impact velocity) required to achieve complete perforation of the plate (Rajput et al. 2018). This peculiar value can be estimated using a practical bilinear approach, as described by Hering et al. (2023), and can provide a solid comparative indicator of the effectiveness of a composite system against impact loads in terms of energy absorption capacity. The different parameters included in the extensive experimental data sets encompass different matrices, different combinations of TRC, with a variety of textile sorts (Hering 2020; Hering et al. 2021), short fiber-reinforced composites (i.e., SHCC) and hybrid composites (i.e., with both short fibers and textile reinforcement) (Signorini et al. 2023).

The data set consists of 193 experiments, with 7 features describing the configuration of the plate and impact. The maximum, minimum, and mean values are displayed for the continuous values in Table 1, while all possible options are shown for the discontinuous values.

The experimental data set is comprehensively visualized in Fig. 1. The distribution of the first two principal components (PCs) for the entire data set is shown in Fig. 1a. PCs are new uncorrelated variables, each representing a linear combination of the original features (as listed in Table 1). They are

Table 1 Description of input *features* and output *label* from the collected data set

Input features [unit]	Min value	Max value	Mean
Matrix type [-]	[TF10, SHCC-LC^3, SHCC-FA]		-
Compressive strength [MPa]	64.9	107.9	97.2
Textile material [-]	[Carbon, Basalt, Glass, Steel Carbon+Glass, Carbon+Dyneema]		-
Number of textile layers [-]	0	4	1
Amount of textile per layer [g/m^2]	0	1026.1	407.1
Mass of plate [kg]	17.9	25.9	23.5
Input impact energy [J]	377.2	7982.9	2614.8
Output label [unit]			
Dissipated energy ΔE [%]	24.3%	100%	66.1%

ordered by the amount of variance they capture, with the first component explaining the most variance. So, this representation clusters experiments with similar input features together while placing experiments with greater differences farther apart. The explained variance of the first two principal components is also annotated in Fig. 1a. A series of experiments with identical material configurations and different impact energies can be identified, appearing along a line with gradually changing dissipated energy. In general, the experiments are closely clustered, with only a few outliers. The distribution of dissipated energy is depicted in Fig. 1b, where most experiments demonstrate 100% energy dissipation.

In detail, for the case study under investigation, the following data sets were implemented for training:

- 169 tests using a plain fine concrete matrix typically adopted for TRC (Pagel, TF10) (159 different textile reinforcements, 10 without any reinforcement) (Hering et al. 2021)
- 12 tests with an SHCC matrix based on a LC^3 binder (6 with 2-ply textile reinforcements, 6 with short fibers only) (Signorini et al. 2023)
- 12 tests with an SHCC matrix with a binder based on fly ash (FA) in partial replacement of Ordinary Portland Cement (OPC) (6 with 2-ply textile reinforcements, 6 with short fibers only) (Signorini et al. 2023).

2.2 Life cycle assessment

The LCA methodology evaluates the environmental impacts of systems, processes, and products from extraction to disposal. As previously mentioned, our study follows its four standardized stages: goal and scope, LCI, LCIA, and interpretation of results.

All composite materials analyzed, including associated quantities, were based on the laboratory-produced samples described in Section 2.1. We used the *LCA for Experts* software, formerly known as GaBi, and its databases for life

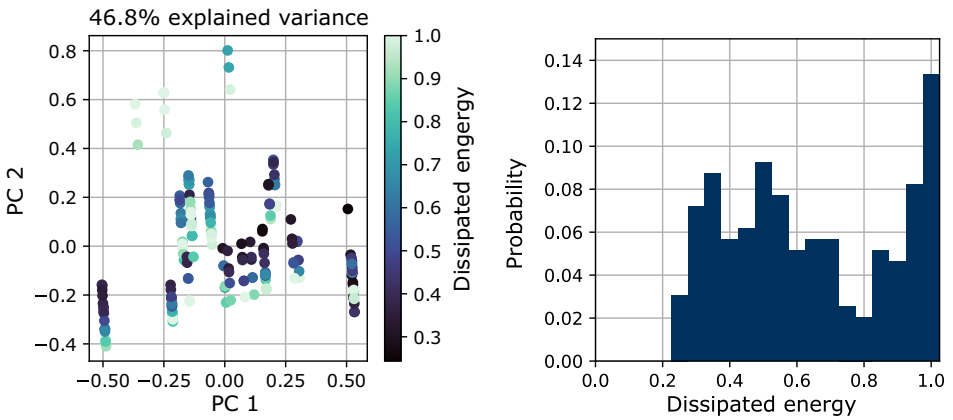

(a) Representation of the standardized input feature space via visualization of the first two principal components. The color of the points represents the output label.

(b) Histogram of output label dissipated energy.

Fig. 1 Experimental dataset visualization

cycle inventory modeling and impact assessment. The data sets adopted refer mainly to Germany, which corresponds to the manufacturing location. The summary of the LCA parameters is shown in Table 2.

2.2.1 Goal and scope

The present work evaluates the environmental performance of SHCC, TRC, and TR-SHCC composites, intended as protective layers of existing RC structures, across different constituent designs. Notwithstanding the complexity of the matter, our evaluation focused solely on quantifying GWP as an indicator of the environmental sustainability of the composites, with the aim of integrating it into the design optimization algorithm. While combining other impact categories, such as resource depletion, human health, and ozone depletion, provides a more comprehensive understanding of environmental impacts and trade-offs, optimizing across multiple metrics adds complexity and makes the approach less practical for use as a tool in material design. GWP was prioritized due to the significant contribution of cement manufacturing to greenhouse gas emissions, particularly from the calcination processes (Humphreys and Mahasenan 2002; Malhotra 2010; Van Den Heede and De Belie 2012). This simplification allowed us to focus on the critical issue associated with cement manufacturing, while future studies could refine the methodology by incorporating and cross-checking multiple indicators.

2.2.2 System boundaries

A cradle-to-practical-completion approach is used, which encompasses raw material extraction (A1), processing and manufacturing (A3), construction and assembly (A5), as well as the transportation to the manufacturing plant (A2) and from suppliers to the project site (A4), as illustrated in Fig. 2. Please note that the material processes sourced from the GaBi databases encompass all relevant steps and technologies up to the factory gate, covering the A1–A3 phases of the supply chain.

2.2.3 Functional unit

The functional unit (FU), defined as the "*quantified performance of a product system*" (International Organization for Standardization 2006b), allows the comparison of the environmental impacts of different systems. Although it is recommended to use more complex functional units that take into account intrinsic properties such as strength and durability (Backes et al. 2023; Panesar et al. 2017), we opted for a volume-based FU of 1 m^3 of composite material to enable direct comparison with other systems in the literature. However, from the perspective of the current case study, the normalization of the volume data to the unit surface of protective layer, i.e., 1 m^2, was embedded in the ML model. In practice, the application of strengthening layers is often expressed in square meters of the existing substrate over which the composite is applied. For this purpose, a nominal thickness of 10 mm for the first layer and 7 mm for subsequent layers of TRC was assumed as far as textile layers are considered. For SHCC, the equivalent of one layer (i.e., 10 mm) is assumed.

2.2.4 Assumptions and limitations

It is important to be aware of certain assumptions and limitations that have an impact on our analysis.

- The decision to limit the system boundaries to cradle-to-practical-completion was based on three important factors. First, owing to the novel nature of the material under assessment, there is a lack of empirical data for the use and end-of-life phases. This lack of data would require the adoption of several assumptions, particularly concerning the service life of the materials. Second, the literature supports the use of a cradle-to-gate approach for TRCs (Williams Portal et al. 2015), SHCCs (Leon-Miquel et al. 2023; Van den Heede et al. 2018; Zhang et al. 2020c), and fiber-reinforced concretes (FRCs) (Stoiber et al. 2021; Ali et al. 2023), as the focus is on identifying materials with the highest environmental burden. A cradle-to-grave assessment is typically performed when the service life of the composite material is considered as one of the functional units (Keoleian et al. 2005; Hajiesmaeili et al. 2019; Habert et al. 2013). Finally, since our work targets the design of the materials themselves, extending the analysis to later stages of the life cycle is not deemed necessary.

- Textiles of the same type may vary in composition, such as fiber density, chemical treatments, or weave

Table 2 Summary of LCA details

Technique	Environmental process-based LCA
Tools	LCA for Experts software (GaBi) v10.8.0.14
Functional unit (FU)	1 m^3 of the composite plate
System boundary	Cradle-to-practical-completion
Impact categories	GWP 100 years (excl. biogenic carbon)

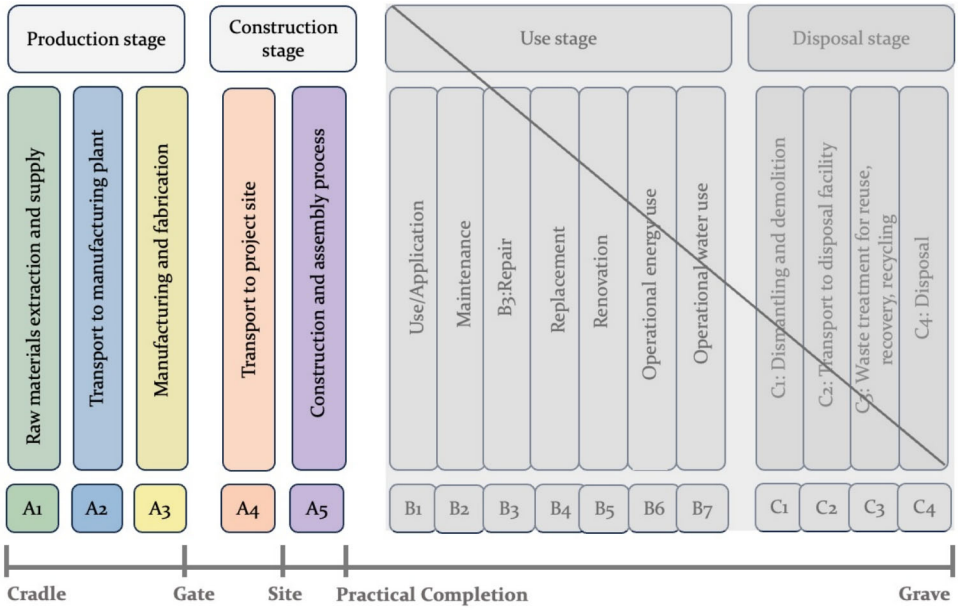

Fig. 2 System boundaries considered for the system under analysis

structure, depending on the supplier. However, these variations are not always captured in the database, where, for example, all glass textiles may be represented by a single process. For carbon reinforcing mesh, we modeled the processes using the Carbon Concrete (C^3-V2.10-I) project, as described by Scope et al. (2020, 2022) as a reference, which provided specific data on supplies, energy requirements, and transport routes for stages A1–A3. In the modeling phase, proxy processes were employed, where corresponding processes were not available in the GaBi databases, and secondary sources such as Environmental Product Declarations (EPDs) were consulted.

2.2.5 Life cycle inventory

Once the system boundaries, functional units, and assumptions are established, the LCI can detail all the flows to model the life cycle of the system. Table 3 lists the materials used, along with their specifications and suppliers.

Material inputs: matrices

Three concrete matrix formulations were used to produce impact-resistant cement-based composites, namely *TF10*, *FA*, and *LC*^{3}, following the nomenclature of Signorini et al. (2023) for similar specimens.

More specifically, TF10 is a pre-mixed dry formula developed by PAGEL Spezial-Beton GmbH & Co. KG (in short, "Pagel"), which is made of OPC type I with 42.5 MPa compressive strength, quartz sand, fly ash, and silica fume. It is the base material for the TRC specimens in our data sets.

The FA and LC^3 formulations, designed for use in SHCCs, consist of type I OPC with a compressive strength of 52.5 MPa, fine-grained quartz sand, and a combination of superplasticizer and viscosity modifying agent (VMA) to enhance rheological properties and ensure uniform fiber dispersion. Both formulations feature a clinker factor of 50%, i.e., half of the binder content consists of SCMs. FA incorporates fly ash as an SCM, while LC^3 uses limestone and calcined clay to reduce the carbon footprint of the binder. Unlike TF10, both mixes also incorporate 2% by volume ultra-high molecular weight polyethylene (UHMWPE) to improve tensile strength and crack control. Further details can be found in the paper by Signorini et al. (2023). It should be noted that TF10 has a lower binder content per unit volume compared to its FA and LC^3 counterparts, as it is specifically designed for TRC and not for SHCC. As a result, coarser aggregates are used (maximum particle size of 1 mm, which is 5 times larger than that of the quartz sand used in SHCC formulations).

Energy consumption

In our construction stage (A5), the calculation of energy consumption is limited to the concrete mixers, owing to our small-scale and laboratory-based production. The energy required to mix concrete is determined by multiplying the energy consumed during a mixing cycle by the duration of the cycle (Ferraris 2001). While factors such as mix type, batch size, and loading method influence energy demands, they were outside the scope of our study.

At the Pagel plant, the dry ingredients are blended, packaged, and shipped to our laboratory site. Although the manufacturer did not provide specific data for this stage, energy consumption was estimated based on the findings of Arularasi et al. (2022), who investigated 15 ready mixes

Table 3 Materials details

Materials	Specification	Supplier(s)
Cement	CEM I 52.5 R-SR3/NA	Holcim Technology Ltd
Fly ash	Steament®H-4	EP Power Minerals GmbH
Calcined clay	Low kaolinitic clay ($\leq 25wt.\%$)	Liapor GmbH & Co.KG
Limestone	Saxodol®	SH minerals GmbH
Calcium sulphate	$CaSO_4 \cdot 12\,H_2O$	Honeywell International Inc
Quartz sand	BCS413	Strobel Quarzsand GmbH
Superplasticizer	MasterGlenium ACE 460	MBCC Group
Viscosity modifier	UW Compound-100	Sika AG
UHMWPE fibers	Dyneema®SK60, 6 mm	EuroFibers BV
Carbon textile	SITGRID, SolGRID	V. FRAAS GmbH
Glass textiles	SSA1363, NWM3	Valmiera glass®and TU Dresden -ITM
Steel textile	Stahlgitter	Dorstener Drahtwerke H. W. Brune & Co. GmbH
Basalt textile	Geogrid 200	Kerakoll GmbH

and found that a typical mixer consumes about 3.5 kW h per cubic meter of concrete. In our laboratory, the dry mix from Pagel is combined with water and superplasticizer. For a batch of 150 ls of fresh concrete, the mixing process consumes 7 kW of power over a 5-min cycle, including drive power, hydraulics, and the mixing drum. This results in an energy consumption of 0.46 kW h per batch or approximately 3.06 kW h per cubic meter of finished product.

Transportation

Transportation for A2 (raw materials to the manufacturing plant) was accounted for within the database processes of the materials. For A4 (transportation to the project site), distances were determined by considering the specific locations of each supplier to our laboratory. To ensure accuracy, we applied the Euro 6 standard, which is the latest and most stringent and rigorous emission regulation in the European Union (European Commission 2012). We also divided the weight classes of the trucks according to the distance: for short and medium distances, we modeled a truck with a total capacity of 12–14 t and a payload of 9.3 t, while for longer distances, we used a heavy truck with a total capacity of 34–40 t and a payload of 27 t.

2.2.6 *Impact assessment*

In the impact assessment phase, environmental inputs and outputs are classified into different impact categories, while characterization factors are used to quantify these impacts into a single score. To quantify and report the carbon footprint of our materials, we followed the Sixth Assessment Report (AR6) of the Intergovernmental Panel on Climate Change (IPCC). The latest AR6 has revised the lifetimes and indirect chemical effects of gases. It now provides more comprehensive emission metrics that distinguish methane (CH_4) from fossil fuel and biogenic sources, with the former being assigned a higher value due to its contribution to CO_2 (IPCC 2022).

Global warming potential

Human activities, particularly the combustion of fossil fuels, have intensified the so-called greenhouse effect. According to the IPCC (2023), concentrations of critical greenhouse gases (namely CO_2, methane, and nitrous oxide) have been steadily increasing. Other gases, such as carbon monoxide and hydrocarbons, indirectly amplify the effect (Harvey 1993). As different pollutants contribute differently to climate change (beyond the mass they release into the atmosphere), the GWP metric helps to standardize this variation by equating each pollutant's contribution to carbon dioxide over a given time horizon. The GWP can be expressed by the ratio in Eq. 1 (IPCC 2021).

$$\mathrm{GWP}_i = \frac{\int_0^T \mathrm{RF}_{\mathrm{CO}_2}(t)\,dt}{\int_0^T \mathrm{RF}_i(t)\,dt} \tag{1}$$

In Eq. 1, GWP_i is the global warming potential of the gas i. $\mathrm{RF}_i(t)$ is the radiative forcing of gas i at time t. $\mathrm{RF}_{\mathrm{CO}_2}(t)$ is the radiative forcing of carbon dioxide at time t. Finally, T is the time horizon over which the GWP is calculated (usually 100 years).

2.3 Machine learning-based optimization

2.3.1 General concepts and principles

The systematic optimization of material property design aims to identify the Pareto front uniformly within a given region. The Pareto front, also known as the Pareto frontier, is an envelope of efficient solutions that considers the best trade-

offs between different sets of input parameters, in our case mechanical performance (dissipated energy) and sustainability index (GWP), without having to consider the full range of parameters involved (Jahan et al. 2016). This approach is known as multi-objective optimization (MOO). To achieve this, a transformation converts the MOO into a sequential single-objective optimization (S-SOO). The S-SOO process is illustrated in Fig. 3. In each iteration, a new plate configuration is evaluated by the ML model to predict the dissipated energy and by the LCA model to calculate the GWP_{100}. These outputs are combined using a scoring function, with the dissipated energy serving as the optimization objective and the GWP_{100} being treated as a constraint. If the constraint is violated, the performance is scored based on the GWP_{100} deviation from the specified limit. MOO is performed through sequential SSO processes, where different maximum allowable GWP_{100} Reference settings are applied. The implementation of the optimization workflow and performance metrics were the scope of a previous publication (Conrad et al. 2024) and briefly recalled here for convenience.

The following scoring function S, which is defined in Eq. 2, was used to evaluate and optimize the plate designs. Here, $Y_{\text{dissipated energy}}$ represents the objective variable and is the output of the ML model. $B_{GWP_{100}}$ denotes the corresponding boundary conditions for the LCA model output $Y_{GWP_{100}}$.

$$S = \begin{cases} Y_{\text{dissipated energy}} & \text{if } Y_{GWP_{100}} \leq B_{GWP_{100}}, \\ Y_{GWP_{100}} - B_{GWP_{100}} & \text{otherwise} \end{cases} \quad (2)$$

The scoring function associated with the *dissipated energy* is based on meeting the GWP limit. If the designed GWP ($Y_{GWP_{100}}$) is within the allowable limit ($B_{GWP_{100}}$), the score S is determined by the design performance ($Y_{\text{dissipated energy}}$). However, if the GWP exceeds the boundary, the score S reflects the deviation from the GWP limit and penalizes the design accordingly. The negation of the scoring function is used as the optimization objective and is defined as

$$\text{Minimize } f(x) = -S(\mathrm{M_{ML}}(x),\ \mathrm{M_{LCA}}(x),\ B_{GWP_{100}}) \quad (3)$$

with x representing the design features of the plate and $\mathrm{M_{ML}}$ the ML model for predicting the dissipated energy and the LCA model $\mathrm{M_{LCA}}$ for calculating the GWP_{100}.

The condition in Eq. 3 allows the optimization algorithm to minimize the score, driving the solution toward satisfying both performance and GWP constraints.

2.3.2 Implementation and input parameters

For the ML modeling of mechanical performance, we used AutoSklearn (v.0.15.0) (Feurer et al. 2015), which was selected for its superior predictive capabilities in materials design, as demonstrated in a previous benchmark study by Conrad et al. (2022). Based on the recommendations of this study, the training time of the AutoSklearn model was configured to be 15 min, using the root mean square error (RMSE) as the scoring metric. This balances sufficient training time for rigorous model optimization with the degradation of predictive performance due to overfitting. In addition, we implemented nested cross-validation to ensure a rigorous evaluation of the model's performance.

The ML model is designed to predict the dissipated energy of composite plates (SHCC, TRC, and TR-SHCC) under specific impact conditions. Therefore, the model takes as input five *features*, namely (i) the number of textile layers, (ii) the weight per unit area of a single textile ply, (iii) the energy input from the impactor, (iv) the constituent material of the continuous fibers in the textile, and (v) the matrix type, the latter two parameters being both represented in one-hot encoded form. The model outputs the predicted dissipated energy (Eq. 4).

$$Y_{\text{dissipated energy}} = \mathrm{M_{ML}}(\text{layers, 1-ply area weight, energy input, textile, matrix}) \quad (4)$$

In order to normalize the performance per unit surface of the protective layer, the plate thicknesses are conventionally specified for the number of plies, as mentioned in Section 2.2.3 describing the functional units for the LCA

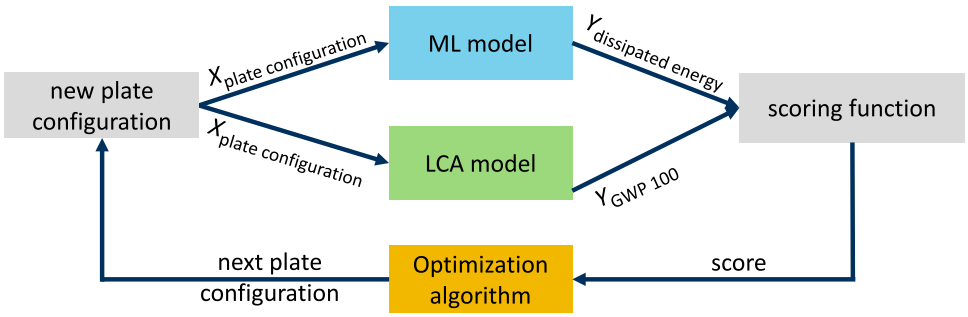

Fig. 3 Overview of the optimization framework

model. In this context, 1 ply corresponds to 10 mm, 2 plies to 17 mm, 3 plies to 24 mm, and 4 plies to 31 mm.

For the optimization process, the GWP_{100} is calculated for each variant considered by the optimization algorithm. First, the GWP of the textile component is determined. Each textile contains a specific mass fraction of impregnation, denoted as $\omega_{coating}$, the production of which has its own inherent environmental impact. The GWP_{100} of the textile is then calculated as the sum of the GWP of the raw textile and the GWP of its impregnation. In addition, the amount of matrix required is estimated based on the volume needed to embed the textile layers. The GWP of the short, dispersed polyethylene fibers in the FA and LC^3 SHCC matrices is included in their formulation.

Finally, the total GWP_{100} for the textile-reinforced concrete plate is obtained by summing the GWP contributions from the textile and the matrix.

To optimize the design for minimal environmental impact, we employed Nevergrad (version 1.0.2) (Rapin and Teytaud 2018), which is based on the covariance matrix adaptation (CMA), an evolutionary algorithm that dynamically adapts a multivariate normal distribution to model the search space. The algorithm iteratively updates the mean and covariance matrix of the distribution based on the performance of candidate solutions (Hansen et al. 2003). By applying the CMA algorithm, we were able to refine the design parameters, such as the number of layers and textile material, to minimize the GWP_{100} while ensuring the required mechanical performance.

3 Results and discussion

3.1 LCA of the fiber-reinforced composites

From the considerable number of mix design combinations considered in this paper, a selection of 13 is presented in Fig. 4, to illustrate and compare their GWP per unit volume. This selection includes two mixes for SHCCs (matrix with short fibers and no textile plies), which have recently been developed as a basis for the impact and blast strengthening of concrete structures (Bracklow et al. 2025), two for hybrid TR-SHCC, including two layers of carbon textile grid, and nine for more conventional TRC, without the inclusion of short fibers.

Binder contribution to GWP in SHCC and TRC-TF10 composites

As expected, the production of the binder, and in particular the OPC clinker, accounted for the most significant contribution to the GWP, affecting up to 72% of the total GWP across the different design scenarios, due to the significant embodied carbon of the production processes of OPC, such as energy-intensive kiln processes, fossil fuel combustion, and clinker formation. The 50% reduction in OPC in the LC^3 and FA cases, where it was replaced by SCMs, resulted in only a modest reduction in GWP. This limited effect is due to the high binder content of SHCC matrices compared to standard TRC matrices (TF10 in our analysis), which use a larger fraction of coarser aggregates. In addition, the thermal processes for calcining clay play a role in the CO_2 balance. However, the incorporation of SCMs has the potential to significantly reduce GHG emissions. This becomes readily apparent when comparing the individual material contributions per kg. In fact, OPC averages 0.845 kg CO_2 eq., while fly ash and calcined clay exhibit significantly lower emissions of 0.196 kg CO_2 eq. and 0.256 kg CO_2 eq., respectively.

Overall, the SHCC matrices entail comparable GWP to the TF10 counterpart at stages A1–A3 (with FA and LC^3 being only 3.52% and 5.81% higher, respectively), despite the substantially different formulation, which is optimized for extreme ductility and damage tolerance for dynamic applications, and thus contains extremely fine aggregates and more binder. The environmental impact in terms of GHG emissions of the SHCC binders must then be weighed against their impact performance, as shown in the following sections. In addition, the use of CEM I 52.5 in the SHCC matrices results in a slightly higher intrinsic GWP per kilogram (0.851 kg CO_2 eq.) than CEM I 42.5 (0.838 kg CO_2 eq.), which is adopted as the main binder in the TF10 formulation.

Influence of fiber type and composite thickness on the environmental impact

Although the matrix plays a crucial role in GWP accounting, the individual contribution of the fiber type must also be considered, as different reinforcements impose varying environmental burdens due to their production processes. When evaluating fibers by their GWP per kilogram, carbon mesh exhibits the highest impact at up to 8.60 kg CO_2-eq/kg, followed by glass mesh at 3.27 kg CO_2-eq/kg and basalt mesh at 2.75 kg CO_2-eq/kg. PE fibers have a lower footprint at 1.79 kg CO_2-eq/kg, while steel mesh have 0.49 kg CO_2-eq/kg.

However, the total GWP contribution of a fiber type depends not only on its unit impact but also on the amount required in the composite, which varies according to the mix design and reinforcement strategy (e.g., to achieve a target mechanical performance). In textile-reinforced composites, a single layer of reinforcement consists of a predefined quantity of fibers per unit area, but the total fiber mass per cubic meter depends on both the number of layers used and the specific reinforcement configuration. In our study, carbon mesh contributes the highest GWP increase per unit volume, with total emissions rising by 125.13 kg CO_2-eq/m^3 when fiber content increases from 7.68 to 22.23 kg/m^3, illustrating how higher reinforcement density amplifies the environmen-

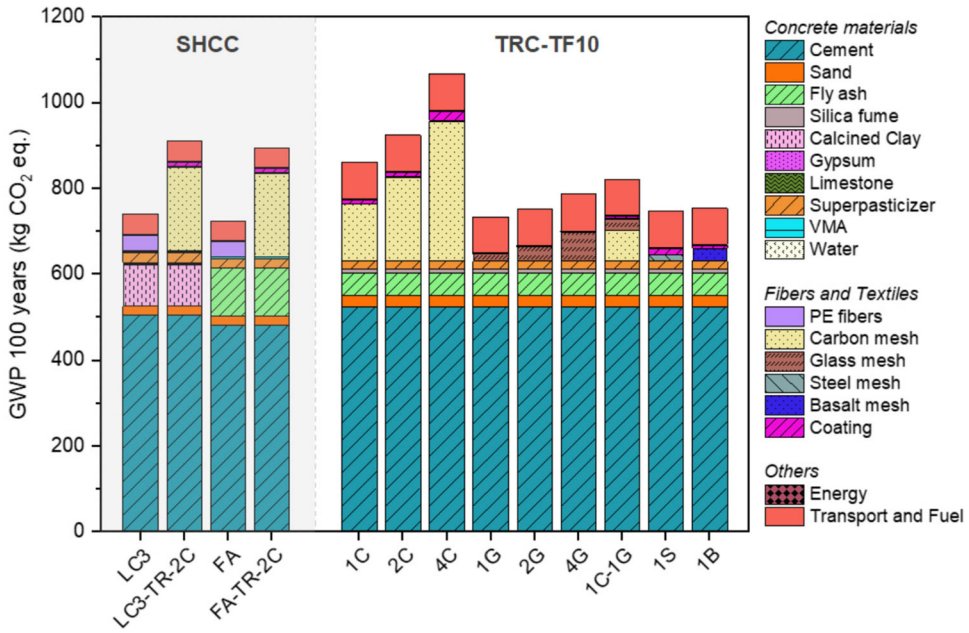

Fig. 4 Comparative analysis of the 100-year global warming potential of the cement-based fiber- and/or textile-reinforced composites. Composites with short fibers are on the left (SHCC and TR-SHCC), with the binder type in the label (FA or LC^3), and TRC combinations with TF10 are clustered on the right. The endings indicate the number of plies (1, 2, or 4) and the type (C=carbon, G=glass, B=basalt, S=steel) of textile

tal impact. Glass mesh shows a smaller variation, with GWP increasing by 9.29 kg CO_2-eq/m^3 when fiber content shifts from 5.21 to 8.05 kg/m^3, underlying its potential as a lower-GWP alternative that maintains effective reinforcement. On the other hand, PE fibers and steel mesh were used at a fixed quantity in the mix design, meaning their GWP contribution remains constant across different configurations. Steel mesh, despite its lower GWP per kilogram, often requires a greater total mass per layer, which can offset its environmental advantage compared to lower-density reinforcements. A similar trend was observed by Backes et al. (2022), who conducted an LCA of TRC reinforced with carbon and glass fibers in a double-wall system and reported 623 kg CO_2 eq. for G-TRC and 791-1079 kg CO_2 eq. for carbon-reinforced composite. In contrast, steel-reinforced concrete exhibited the highest impact (1369 kg CO_2eq with blast furnace steel). These findings align with our results that carbon textiles have the highest per-unit GWP, while glass fiber textiles represent a lower impact alternative.

This distinction becomes even more apparent when analyzing the total GWP contribution per unit volume. Due to the energy-intensive production of carbon fibers, the use of four textile plies, regardless of the matrix considered, implies a significant environmental impact compared to 1-ply or 2-ply counterparts and should only be considered for special applications with extremely high strength requirements. On the contrary, the use of glass textiles brings about significantly lower emissions due to the less energy-intensive production process and the lower grade of the raw materials. In fact, the number of textile layers plays a minor role in G-TRC; the emissions of SHCC specimens containing only PE short fibers as reinforcement are comparable.

The results, ranked from the most to the least environmentally favorable mix design, are presented in Table 4, which provides GWP per square meter (kg CO_2 eq m^{-2}), which accounts for the influence of plate thickness based on the number of textile reinforcement layers. This distinction is important, as the actual environmental impact per unit area depends not only on material composition but also on structural requirements, which dictate necessary thickness adjustments. It should be noted, however, that these partial results completely neglect the mechanical performance of the composites, which will be addressed and weighed in the following sections.

The results emphasize that material sustainability cannot be judged on per m^3 emissions alone. While cement-intensive SHCC formulations rank higher in GWP per volume, they may remain competitive at the structural level when reinforcement strategies minimize overall material use. Similarly, while hybrid configurations increase binder demand, their superior performance enables thinner sections, reducing material consumption per unit area. This reinforces the importance of evaluating sustainability through a combined volumetric and structural lens rather than relying on isolated material emissions.

Table 4 Design configurations in ascending order of GWP per m^3 of composite, measured in kg CO_2 eq

Matrix	Fibers	Textile	Layers	Composite	GWP/1 m^3	GWP/1 m^2
FA	UHMWPE	–	–	SHCC	722.82	7.23
TF10	–	Glass	1	TRC	734.26	7.34
LC^3	UHMWPE	–	–	SHCC	740.55	7.41
TF10	–	Steel	1	TRC	748.37	7.48
TF10	–	Glass	2	TRC	752.10	12.79
TF10	–	Basalt	1	TRC	754.12	7.54
TF10	–	Glass	4	TRC	787.00	24.40
TF10	–	Carbon+Glass	2	TRC	822.13	13.98
TF10	–	Carbon	1	TRC	861.35	8.61
FA	UHMWPE	Carbon	2	TR-SHCC	894.89	15.21
LC^3	UHMWPE	Carbon	2	TR-SHCC	912.62	15.51
TF10	–	Carbon	2	TRC	925.14	15.73
TF10	–	Carbon	4	TRC	1067.81	33.10

The table also includes GWP per m^2, factoring in the varying plate thicknesses depending on the number of textile layers

3.2 Optimized designs: identification of trade-offs between mechanical performance and sustainability credentials

Optimizing fiber-reinforced composites requires balancing mechanical performance with environmental impact, as improving one aspect often comes at the expense of the other. Higher mechanical efficiency is typically associated with greater material consumption, leading to increased emissions, particularly due to cement and carbon textiles. Conversely, reducing GWP by selecting low-impact materials can compromise energy dissipation and durability, limiting their applicability in impact-resistant structures. To better understand these trade-offs, we analyzed the sensitivity of configuration parameters to both dissipated energy and GWP using SHAP (Shapley additive explanations) (Lundberg and Lee 2017). SHAP quantifies the contribution of each input feature to the model's predictions, providing insights into feature importance. The analysis revealed that the most influential features for the dissipated energy related to plate configuration, ranked from most to least relevant, are the number of layers, matrix type, textile type, and 1-ply area weight. For GWP, the ranking is number of layers, textile type, 1-ply area weight, and matrix type. Notably, more layers and an increased 1-ply area weight contribute to higher dissipated energy and GWP, underscoring the inherent trade-offs in composite design. To assess the real-world implications of these trade-offs, our case study focuses on three distinct impact scenarios, namely 2000 J, 4000 J, and 6000 J of minimum input energy, to assess how the optimal design of the cement-based protective composites varies across different levels of severity. To give an example, a 12/70 projectile fired from a distance of 5 m would deliver an impact energy of approximately 4000 J (Dapper et al. 2021).

For the lowest impact range, 2000 J, the optimization indicates that the complete energy dissipation of the input energy can be achieved by the SHCC protective plates with short fibers only, without the need for any textile reinforcement. The distributed microcracks efficiently absorb impact energy, making additional reinforcement unnecessary at this energy level. However, as the impact energy increases to 4000 J and 6000 J, hybrid TR-SHCC and TRC configurations become necessary to meet mechanical demands. The results are presented in Figs. 5 and 7, respectively. In both figures, the optimized design fronts are connected in green, with further differentiation based on the textile material: blue circles represent carbon meshes, and purple crosses represent glass textiles. When the green line overlaps with the blue circles or purple crosses, it indicates that the optimized design uses the corresponding textile material at that specific location. The table below the figures shows the optimal configuration in terms of matrix type, textile material, and number of layers.

All experimental points from the database with impact energies equal to or greater than 4000 J and 6000 J are displayed in their respective graphs. Experimental data for configurations that include textile layers (i.e., TRC and TR-SHCC) are plotted as gray points, while those for SHCC (i.e., without textile reinforcement) are plotted as orange points. The Pareto optimal points are connected by lines to illustrate the trade-offs between energy dissipation and GWP_{100}. Notably, the predicted optimized designs consist of SHCC with a single textile layer, which outperform the experimental database, although the single-layer designs with SHCC matrices (FA and LC^3) were not tested in the experiments.

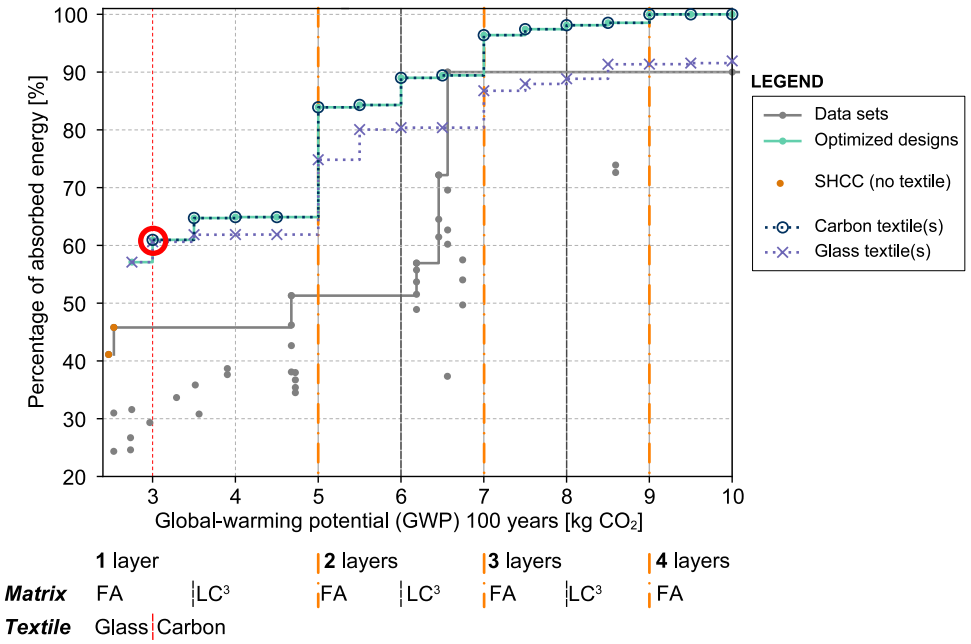

Fig. 5 Results for the optimized designs for an impact energy of 4000 J. The optimum configurations for the parameters layers, matrix, and textiles are displayed below the graph. The red circle indicates the transition point between optimal designs using carbon and glass textiles

Moderate impact scenario (4000 J)

As shown in Fig. 5, the optimized design can dissipate nearly 90% of the input energy with a GWP of 6 kg CO_2 eq. The corresponding configuration consists of a hybrid TR-SHCC composite with 2 layers of carbon textile and an LC^3 SHCC matrix. For the same GWP level, the best configuration with glass textiles is able to dissipate about 80% of the input kinetic energy using 2 layers. Notably, the best configuration in our experimental database was able to achieve just over 50% of energy dissipation only. This discrepancy serves as a reminder that even carefully designed experimental programs may fall short of optimization and that ML can play an important role in guiding material selection and design.

In general, for the impact energy of 4000 J, the optimized designs improve the entire Pareto front compared to the known designs until the database entries achieve a 100% energy dissipation, at which point further improvement is no longer possible. However, it is still possible to find a design that achieves full energy absorption with a considerably lower GWP.

(i) Textile materials and number of layers. As expected, due to its superior mechanical properties, carbon outperforms glass, steel, and basalt among the textiles studied and is generally the optimal choice for impact protection. However, when strict GHG emission limits are imposed (in our case, a GWP_{100} below 2.8 kg), carbon can no longer meet this requirement, making glass the preferred option over steel and basalt. However, these low-emission scenarios are less relevant to our study of impact protection, where high energy from collisions, blasts, and extreme events requires high toughness. In contrast, glass and basalt may offer a better compromise for retrofitting masonry structures under conventional loading conditions. In fact, while carbon clearly offers a higher mechanical performance compared to glass for the same 1-ply area weight, this advantage diminishes when an upper limit is imposed on the GWP_{100}. Under such a constraint, a higher 1-ply area weight can be used for glass textiles, partially compensating for the performance difference. However, as the matrix is the primary determinant of the GWP_{100} of the composite system, the increase in matrix material required to accommodate multiple glass textile layers to match the mechanical performance of a single carbon ply reduces the sustainability attractiveness of using multiple glass textiles.

A further increase of the dissipated energy can be obtained by increasing the 1-ply area weight of the given textile. The optimized designs are characterized by an increasing 1-ply area weight with a higher limit of GWP_{100}, up to the point where a higher number of layers or a different matrix can be used. Although adding reinforcement layers improves energy dissipation, the GWP impact does not increase linearly. For instance, transitioning from a single textile layer to two layers significantly enhances mechanical performance, but beyond a certain threshold, the sustainability cost outweighs the performance gains.

(ii) Matrix. The matrices composition influences key properties such as crack-bridging ability, fiber dispersion, and overall energy dissipation. In the context of impact-resistant composites, the challenge lies in optimizing the binder for-

mulation to achieve high toughness while maintaining low GWP. Among the matrices, within the same GWP_{100} limit, the FA-based SHCC allows for higher textile incorporation compared to LC^3-SHCC, which requires a slightly higher cement content. However, when LC^3-SHCC meets the GWP constraints of the design, it is preferred due to its superior performance. SHCC-FA is considered a secondary option, chosen only when the LC^3-based configuration cannot meet the GWP_{100} requirement. It is worth noting that both matrix compositions are still under development, with ongoing research aimed at further reducing the cement content in LC^3 binders (Ahmed et al. 2023) and exploring the use of low-grade fibers (Ahmed et al. 2024). In addition, the availability of fly ash is being reduced as coal plants are phased out.

(iii) Combined influence of fiber-matrix on sustainability trade-offs. When comparing SHCC and hybrid TR-SHCC protective composites with conventional TRC, Pagel TF10 is never the preferred matrix due to its inferior impact performance, although as plain concrete it exhibits a better environmental score than SHCC matrices. This highlights the advantages of combining short and continuous fibers in dissipating energy from extreme dynamic loads (Yoo et al. 2015; Liu et al. 2018; Signorini et al. 2023). The synergistic effect of these fibers outweighs the additional GWP associated with the higher binder content in SHCC and hybrid composites compared to conventional fine-grained concrete for TRC, ultimately contributing to improved impact safety and sustainability. This is further illustrated in Fig. 6, which compares relevant material combinations in terms of GWP and ballistic limit.

The percentages in Fig. 6 refer to TRC with Pagel TF10 matrix, two carbon plies, and no short fibers. As observed, FA-SHCC and LC^3-SHCC reduce emissions significantly ($\Delta GWP = -54\%$ and $\Delta GWP = -53\%$) while improving ballistic performance ($\Delta E_{bl} = +26\%$ and $\Delta E_{bl} = +34\%$) due to fiber bridging, though not to the level of hybrid configurations. However, for moderate impact energy scenarios, SHCC combinations can obviate the need for carbon textiles. Hybrid TR-SHCC composites (FA-TR-SHCC and LC^3-TR-SHCC) achieve the highest impact resistance ($\Delta E_{bl} = 145\%$ and $\Delta E_{bl} = 148\%$) but maintain GWP levels close to TRC ($\Delta GWP = -3\%$ and $\Delta GWP = -1\%$). On the other hand, TF10-2G with glass textiles offers a moderate balance ($\Delta E_{bl} = +17\%$, $\Delta GWP = -19\%$) and appears to be a viable option in replacement of carbon textiles.

Given these performance and emission trends, material selection depends on the required level of impact resistance. When higher design toughness is required, hybrid composites, despite having a similar GWP to TRC, show remarkable improvements in mechanical performance, allowing for lower material consumption.

Severe impact scenario (6000 J)

The optimized designs demonstrate significant improvement across the entire Pareto front compared to experimental designs, although achieving 100% energy dissipation in such a high-impact scenario is not feasible, likely resulting in composite perforation. The best performing designs closely resemble those from the 4000 J case. In contrast, glass reinforcement partially outperforms carbon in scenarios with low

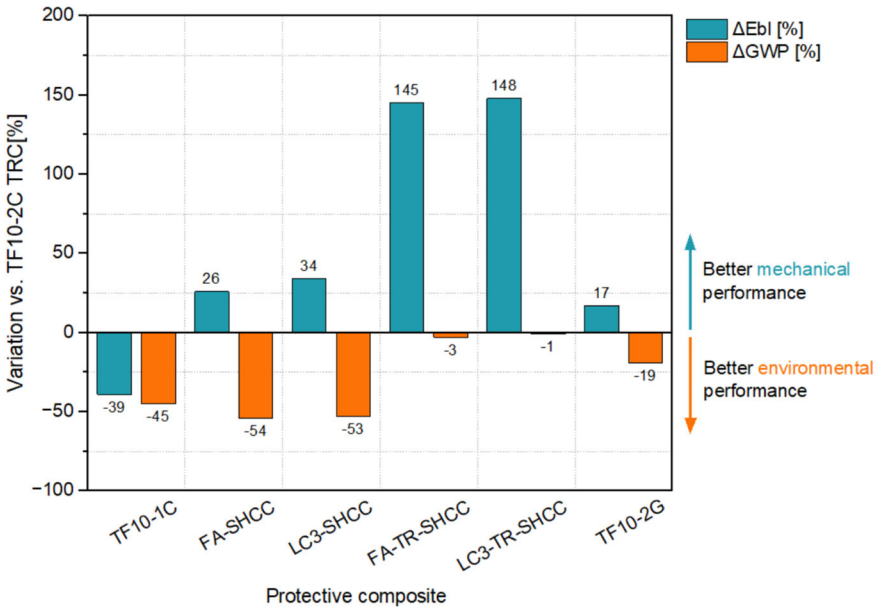

Fig. 6 Combined view of the variation of GWP emissions (ΔGWP) and ballistic limit (ΔE_{bl})) for different material combinations in comparison with TRC (TF10 matrix and 2 plies of carbon textile). Data for ballistic limit calculation are retrieved by Hering et al. (2023) and Signorini et al. (2023)

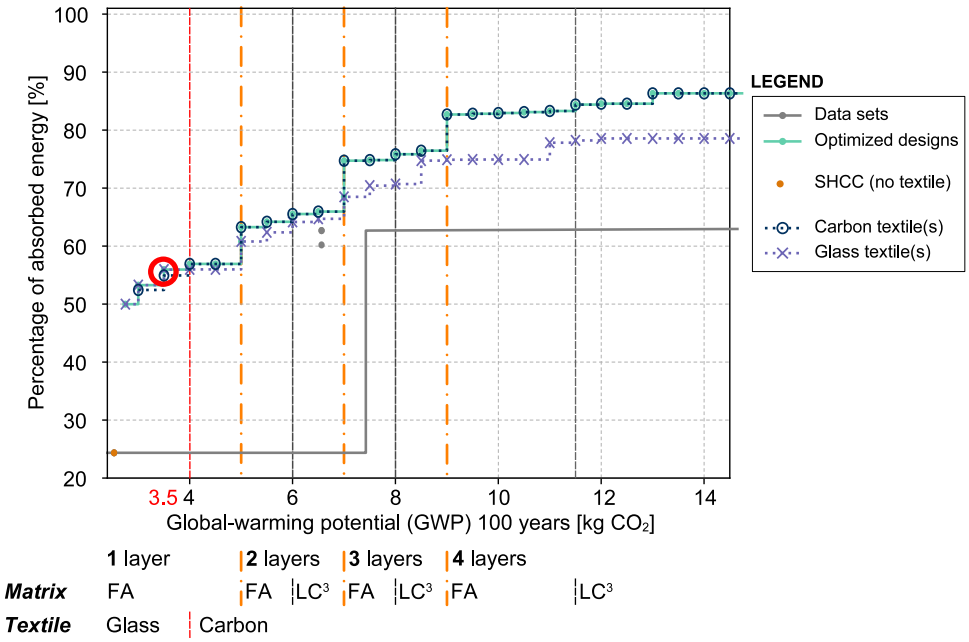

Fig. 7 Results for the optimized designs for an impact energy of 6000 J. The optimum configurations for the parameters layers, matrix, and textiles are displayed below the graph

GWP scenarios up to 3.5 kg. This can be attributed to the need for more textile reinforcement at high impact energies, and since glass textiles have a lower GWP_{100}, a higher 1-ply area weight with more fibers can be used compared to carbon (Fig. 7).

However, the ML model in this area is negatively affected by the sparse data for such high impacts, which could impair the accuracy of the prediction. In any case, it is paramount to understand that the designer must interpret the results of the ML model on an individual basis at each level of investigation, from laboratory research to field application (Pearce et al. 1995; Fröderberg 2015).

4 Conclusions and outlook

With the aim of combining performance and sustainability criteria in the selection and design process of construction materials, we have developed a simple but effective integrated framework based on an advanced machine learning approach that links experimental data sets and corresponding material properties with life cycle assessment concepts. A specific design scenario is considered based on a database on the impact performance of fiber- and/or textile-reinforced mineral-bonded composites designed for structural protection of existing concrete members vulnerable to impact loads. The LCA was embedded in terms of global warming potential, as this is considered to be one of the most sensitive and critical environmental parameters in the concrete industry. From this case study, the following considerations can be formulated:

- Cement production is the primary contributor to the GWP of fiber-reinforced composites. Several strategies can help reduce embodied carbon in construction, including resource efficiency, low-carbon materials, circular approaches, and a holistic material-climate-waste framework. We show that replacing clinker—the most carbon-intensive component of cement—with supplementary cementitious materials, especially highly available ones such as limestone and calcined clay, is effective.
- Once the ML model was trained on the experimental data set, it was able to estimate the energy absorption of untested material combinations. The design configurations were optimized for target input impact energies of 2000 J, 4000 J, and 6000 J. For the mildest scenario, the model confirmed that SHCC with short fibers alone could fully dissipate the impact energy, eliminating the need for textile reinforcement. At 4000 J, the ML approach revealed that a hybrid TR-SHCC composite with two layers of carbon textile and an LC^3-based SHCC matrix could achieve nearly 90% energy dissipation while maintaining a GWP of approximately 6 kg CO_2 eq., outperforming the best configurations in the experimental dataset, which achieved just over 50%. For extreme impact scenarios (6000 J), the model noted the need for further reinforcement and that optimized textile arrangements could effectively mitigate perforation,

although the achievement of full energy dissipation was not feasible.

- Among the optimized designs, hybrid composites containing both short fibers and textile plies proved to be the most effective for the target application. Most notably, the higher GWP of SHCC matrices, associated with higher binder content compared to conventional matrices designed for textile-reinforced concrete, is more than offset by the gain in toughness. This synergistic behavior minimizes brittle failure, distributes impact loads more effectively, and reduces stress concentrations within the composite. In addition, the approach with hybrid fiber reinforcement optimizes material utilization by reducing the number of textile layers required, resulting in lower material consumption while maintaining mechanical performance. Ultimately, these characteristics make hybrid composites an optimal choice in the design of protective structures, even as far as sustainability credentials are concerned.
- Although carbon textiles contributed the highest GWP per cubic meter of composite, far exceeding glass, steel, and basalt counterparts, they offered significantly superior mechanical performance. This implies that a high dissipation capacity can be achieved with a significantly lower number of plies, thereby reducing the thickness and the amount of matrix required, which also results in a lower overall composite mass—an important factor for lightweight structural applications. Furthermore, the long-term durability of carbon textiles extends the structural lifespan of protective elements, minimizing maintenance needs and further offsetting their initial environmental impact. Therefore, trade-offs must be considered, and for this case study, carbon textiles represent the optimal solution.
- Nevertheless, where GWP limits are stringent, glass appears to be the preferred option, as the emissions associated with carbon textiles cannot fall below a certain threshold. In general, lower-strength textiles could be preferred over carbon textiles in several case studies where lower mechanical performance is required.

Ultimately, the balance between performance and environmental impact depends on specific application needs and priorities. Integrating these considerations highlights the importance of assessing both mechanical and sustainability factors, as their absolute values do not provide a complete picture. Furthermore, while these are valid tools to assist researchers and practitioners in the design and selection of materials, the human factor is still essential in the final decision-making.

The results of this study on the optimization of fiber-reinforced cement-based composites have broader methodological and practical implications beyond impact-resistant materials. Theoretically, the integration of ML and LCA into a MOO framework establishes a scalable, data-driven methodology for balancing structural performance and sustainability, replacing conventional trial-and-error design with AI-driven trade-off exploration. The results further highlight the potential of hybrid reinforcement strategies, showing that optimized TR-SHCC composites can outperform traditional TRC in both impact absorption and environmental impact, with applications in resilient infrastructure and disaster mitigation.

In practical terms, the study provides clear guidance on when to prioritize fibers with higher tensile strength and energy dissipation for severe impacts and when to opt for lower-carbon alternatives with sufficient toughness for moderate protection. By identifying optimal reinforcement configurations, the study enables cost-effective designs that reduce material waste while maintaining or enhancing structural integrity.

As these results represent a preliminary framework, ongoing research aims to optimize the ML model to include various LCA parameters and a comprehensive variety of case scenarios, as well as to validate the approach with additional retrospective experiments. Future research will focus on

- Expanding the optimization objective function to include additional LCA indicators such as embodied energy, water footprint, and toxicity potential.
- Enhancing ML models to improve prediction accuracy and generalization across different material systems.
- Conducting further validation through retrospective experimental studies and real-world case applications.

Glossary of key terms

- **ANN**: Artificial neural network
- **FU**: Functional unit
- **FRC**: Fiber reinforced concrete
- **GWP**: Global warming potential
- **IPCC**: Intergovernmental Panel on Climate Change
- **LCA**: Life cycle assessment
- **LC^3**: Limestone calcined clay cement
- **LCI**: Life cycle inventory
- **LCIA**: Life cycle impact assessment
- **ML**: Machine learning
- **OPC**: Ordinary Portland Cement
- **RC**: Reinforced concrete
- **SCM**: Supplementary cementitious materials
- **SHCC**: Strain-hardening cementitious composite
- **TRC**: Textile reinforced concrete
- **TR-SHCC**: Textile reinforced SHCC

- **UHMWPE**: Ultra-high-molecular-weight polyethylene

Acknowledgements The financial support of the German Research Foundation (Deutsche Forschungsgemeinschaft, DFG) within the Research Training Group (Graduiertenkollegs, GRK) 2250 "Mineral-bonded composites for enhanced structural impact safety" (grant no. 287321140) is gratefully acknowledged.

Author Contributions Isabela de Paula Salgado: conceptualization, methodology, validation, formal analysis, investigation, data curation, writing—original draft, visualization. Felix Conrad: conceptualization, methodology, software, validation, formal analysis, investigation, data curation, writing—original draft, visualization. Cesare Signorini: conceptualization, methodology, validation, formal analysis, investigation, writing—original draft, writing—review and editing, visualization, supervision, project administration. Edeltraud Günther: methodology, validation, resources, writing—review and editing, supervision, funding acquisition. Steffen Ihlenfeldt: methodology, resources, writing—review and editing, supervision, funding acquisition. Viktor Mechtcherine: resources, writing—review and editing, supervision, funding acquisition.

Funding Open Access funding enabled and organized by Projekt DEAL.

Data Availability Data will be made available upon reasonable request.

Declarations

Conflict of interest The authors declare no competing interests.

References

Aggarwal C, Molleti S, Ghobadi M (2024) A comprehensive review of life cycle assessment (LCA) studies in roofing industry: current trends and future directions. Smart Cities 7(5):2781–2801. https://doi.org/10.3390/smartcities7050108

Ahmed AH, Nune S, Liebscher M et al (2023) Exploring the role of dilutive effects on microstructural development and hydration kinetics of limestone calcined clay cement (LC^3) made of low-grade raw materials. J Clean Prod 428:139438. https://doi.org/10.1016/j.jclepro.2023.139438

Ahmed AH, Signorini C, Chikhradze M et al (2024) Employing limestone and calcined clay for preserving the strain-hardening response of PET fiber-reinforced cementitious composites. Constr Build Mater 438:137166. https://doi.org/10.1016/j.conbuildmat.2024.137166

Ali B, Ahmed H, Hafez H et al (2023) Life cycle impact assessment (cradle-to-gate) of fiber-reinforced concrete application for pavement use: a case study of Islamabad City. Int J Pavement Res Technol 16(2):247–263. https://doi.org/10.1007/s42947-021-00129-8

Anand CK, Amor B (2017) Recent developments, future challenges and new research directions in LCA of buildings: a critical review. Renew Sust Energ Rev 67:408–416. https://doi.org/10.1016/j.rser.2016.09.058

Anwar GA, Dong Y, Li Y (2020) Performance-based decision-making of buildings under seismic hazard considering long-term loss, sustainability, and resilience. Struct Infrastruct Eng 17(4):454–470. https://doi.org/10.1080/15732479.2020.1845751

Arularasi V, Pachiappan T, Avudaiappan S et al (2022) Effects of admixtures on energy consumption in the process of ready-mixed concrete mixing. Materials 15(12):4143. https://doi.org/10.3390/ma15124143

Asadi Shamsabadi E, Salehpour M, Zandifaez P et al (2023) Data-driven multicollinearity-aware multi-objective optimisation of green concrete mixes. J Clean Prod 390:136103. https://doi.org/10.1016/j.jclepro.2023.136103

Azari R, Garshasbi S, Amini P et al (2016) Multi-objective optimization of building envelope design for life cycle environmental performance. Energy Build 126. https://doi.org/10.1016/j.enbuild.2016.05.054

Backes JG, Scheurer M, Kalthoff M et al (2022) Sustainability of textile reinforcements for carbon concrete – today and tomorrow. In: fib Symposium, pp 2130–2138. https://www.scopus.com/inward/record.uri?eid=2-s2.0-85143899807&partnerID=40&md5=fd5f376e86afd167e1e2b7e5fe7d3058

Backes JG, Hinkle-Johnson R, Traverso M (2023) The influence of the functional unit on the comparability of life cycle assessments in the construction sector: a systematic literature review and attempt at unification for reinforced concrete. Case Stud Constr Mater 18:e01966. https://doi.org/10.1016/j.cscm.2023.e01966

Belaïd F (2022) How does concrete and cement industry transformation contribute to mitigating climate change challenges? Resources. Conserv Recycl Adv 15:200084. https://doi.org/10.1016/j.rcradv.2022.200084

Bleischwitz R, Spataru C, VanDeveer SD et al (2018) Resource nexus perspectives towards the United Nations sustainable development goals. Nat Sustain 1(12):737–743. https://doi.org/10.1038/s41893-018-0173-2

Bracklow F, Jackson CM, Signorini C, Jacques E, Beckmann B, Curbach M, Mechtcherine V (2025) Hybrid mineral-bonded protective layers for enhanced self-centering capacity of reinforced concrete beams subjected to blast. Eng Struct 322:119151. https://doi.org/10.1016/j.engstruct.2024.119151

Bueno C, Hauschild MZ, Rossignolo JA et al (2016) Sensitivity analysis of the use of life cycle impact assessment methods: a case study on building materials. J Clean Prod 112:2208–2220. https://doi.org/10.1016/j.jclepro.2015.10.006

Chaudhury R, Sharma U, Thapliyal P et al (2023) Low-CO_2 emission strategies to achieve net zero target in cement sector. J Clean Prod 137466. https://doi.org/10.1016/j.jclepro.2023.137466

Conrad F, Mälzer M, Schwarzenberger M et al (2022) Benchmarking AutoML for regression tasks on small tabular data in materials design. Sci Rep 12(1):19350. https://doi.org/10.1038/s41598-022-23327-1

Conrad F, Stöcker J, Signorini C et al (2024) Exploring design space: machine learning for multi-objective materials design optimization with enhanced evaluation strategies. Comput Mater Sci 113432. https://doi.org/10.1016/j.commatsci.2024.113432

D'Amico A, Ciulla G, Traverso M et al (2019) Artificial neural networks to assess energy and environmental performance of buildings: an

Italian case study. J Clean Prod 239. https://doi.org/10.1016/j.jclepro.2019.117993
D'Amico B, Myers RJ, Sykes J et al (2019) Machine learning for sustainable structures: a call for data. Structures 19. https://doi.org/10.1016/j.istruc.2018.11.013
Dapper PR, Ehrendring HZ, Pacheco F et al (2021) Ballistic impact resistance of UHPC plates made with hybrid fibers and low binder content. Sustainability 13(23):13410. https://doi.org/10.3390/su132313410
de Paula Salgado I, Günther E, Mechtcherine V (2025) Integrated sustainability and resilience assessments of concrete infrastructures subjected to hazards: a systematic literature review. Sustain Resilient Infrastruct. https://doi.org/10.1080/23789689.2025.2471119
Derissen S, Quaas MF, Baumgärtner S (2011) The relationship between resilience and sustainability of ecological-economic systems. Ecol Econ 70(6):1121–1128. https://doi.org/10.1016/j.ecolecon.2011.01.003
Ding Y, Yu K, Li M (2022) A review on high-strength engineered cementitious composites (HS-ECC): design, mechanical property and structural application. In: Structures. Elsevier, pp 903–921. https://doi.org/10.1016/j.istruc.2021.10.036
Donnini J, Signorini C, Corinaldesi V et al (2024) Use of recycled and virgin carbon fibers in limestone calcined clay cement composites. In: RILEM-fib international symposium on fibre reinforced concrete. Springer, pp 75–82. https://doi.org/10.1007/978-3-031-70145-0_10
Duprez S, Fouquet M, Herreros Q et al (2019) Improving life cycle-based exploration methods by coupling sensitivity analysis and metamodels. Sustain Cities Soc 44. https://doi.org/10.1016/j.scs.2018.09.032
Ebekozien A, Aigbavboa C, Aigbedion M (2023) Construction industry post-COVID-19 recovery: stakeholders perspective on achieving sustainable development goals. Int J Constr Manag 23(8):1376–1386. https://doi.org/10.1080/15623599.2021.1973184
European Commission (2012) Commission regulation (EU) no 459/2012 of 29 may 2012 amending regulation (EC) no 715/2007 of the European parliament and of the council and commission regulation (EC) no 692/2008 as regards emissions from light passenger and commercial vehicles (euro 6)
Ferraris CF (2001) Concrete mixing methods and concrete mixers: state of the art. J Res Nat Inst Stand Technol 106(2):391. https://doi.org/10.6028/jres.106.016
Feurer M, Klein A, Eggensperger K et al (2015) Efficient and robust automated machine learning. In: Cortes C, Lawrence ND, Lee DD, et al (eds) Advances in neural information processing systems, vol 28. Curran Associates, Inc., pp 2962–2970
Fröderberg M (2015) Conceptual design strategy: appraisal of practitioner approaches. Struct Eng Int 25(2):151–158. https://doi.org/10.2749/101686614X14043795570615
Ghoroghi A, Rezgui Y, Petri I et al (2022) Advances in application of machine learning to life cycle assessment: a literature review. Int J Life Cycle Assess 27(3). https://doi.org/10.1007/s11367-022-02030-3
Habert G, Denarié E, Šajna A et al (2013) Lowering the global warming impact of bridge rehabilitations by using ultra high performance fibre reinforced concretes. Cem Concr Compos 38:1–11. https://doi.org/10.1016/j.cemconcomp.2012.11.008
Hajiesmaeili A, Pittau F, Denarié E et al (2019) Life cycle analysis of strengthening existing RC structures with R-PE-UHPFRC. Sustainability 11(24):6923. https://doi.org/10.3390/su11246923
Hanaoka K (2021) Bayesian optimization for goal-oriented multi-objective inverse material design. iScience 24(7):102781. https://doi.org/10.1016/j.isci.2021.102781
Hansen N, Müller SD, Koumoutsakos P (2003) Reducing the time complexity of the derandomized evolution strategy with covariance matrix adaptation (CMA-ES). Evol Comput 11(1):1–18. https://doi.org/10.1162/106365603321828970
Harvey LD (1993) A guide to global warming potentials (GWPs). Energy Policy 21(1):24–34. https://doi.org/10.1016/0301-4215(93)90205-T
He S, Mustafa S, Chang Z et al (2023) Ultra-thin strain hardening cementitious composite (SHCC) layer in reinforced concrete cover zone for crack width control. Eng Struct 292:116584. https://doi.org/10.1016/j.engstruct.2023.116584
Hering M (2020) Investigation of mineral-bonded reinforcement layers for reinforced concrete slabs against impact loads. Phd thesis, Technical University of Dresden, Dresden. https://nbn-resolving.org/urn:nbn:de:bsz:14-qucosa2-737908. Published version
Hering M, Kühn T, Curbach M (2021) Small-scale plate tests with fine concrete in experiment and first simplified simulation. Struct Concr 22(2):637–649. https://doi.org/10.1002/suco.201900333
Hering M, Sievers J, Curbach M et al (2023) An approach to predicting the ballistic limit of thin textile-reinforced concrete plates based on experimental results. Buildings 13(9):2234. https://doi.org/10.3390/buildings13092234
Huang Y, Zhang J, Tze Ann F et al (2020) Intelligent mixture design of steel fibre reinforced concrete using a support vector regression and firefly algorithm based multi-objective optimization model. Constr Build Mater 260:120457. https://doi.org/10.1016/j.conbuildmat.2020.120457
Humphreys K, Mahasenan M (2002) Towards a sustainable cement industry. Substudy 8: climate change
Imbabi MS, Carrigan C, McKenna S (2012) Trends and developments in green cement and concrete technology. Int J Sustain Built Environ 1(2):194–216. https://doi.org/10.1016/j.ijsbe.2013.05.001
International Organization for Standardization (2006a) ISO 14040. Environmental management - life cycle assessment - principles and framework. Geneva, Switzerland. https://www.iso.org/standard/38498.html
International Organization for Standardization (2006b) ISO 14044. Environmental management - life cycle assessment - requirements and guidelines. Geneva, Switzerland. https://www.iso.org/standard/38498.html
IPCC (2021) Climate change 2021: the physical science basis. Contribution of working group i to the sixth assessment report of the intergovernmental panel on climate change. Cambridge University Press, Cambridge, UK and New York, NY, USA. https://doi.org/10.1017/9781009157896
IPCC (2022) Climate change 2022: mitigation of climate change. Contribution of working group III to the sixth assessment report of the intergovernmental panel on climate change. Cambridge University Press, Cambridge, UK and New York, NY, USA, https://doi.org/10.1017/9781009157926
IPCC (2023) Climate change 2023: synthesis report. Contribution of working groups I, II and III to the sixth assessment report of the intergovernmental panel on climate change. IPCC, Geneva, Switzerland. https://doi.org/10.59327/IPCC/AR6-9789291691647.001
Jahan A, Edwards KL, Bahraminasab M (2016) Multi-criteria decision analysis for supporting the selection of engineering materials in product design. Butterworth-Heinemann
Keoleian GA, Kendall A, Dettling JE et al (2005) Life cycle modeling of concrete bridge design: comparison of engineered cementitious composite link slabs and conventional steel expansion joints. J Infrastruct Syst 11(1):51–60. https://doi.org/10.1061/(ASCE)1076-0342(2005)11:1(51)
Kühn T, Curbach M (2015) Behavior of RC-slabs under impact-loading. In: EPJ web of conferences. EDP Sciences, p 01062. https://doi.org/10.1051/epjconf/20159401062
Leon-Miquel M, Silva-Retamal J, Aparicio D et al (2023) Novel application of Chilean natural pozzolan for sustainable strain-hardening

cementitious composite. Resour Conserv Recycl 197:107098. https://doi.org/10.1016/j.resconrec.2023.107098

Li J, Zhang W, Li C et al (2019) Green concrete containing diatomaceous earth and limestone: workability, mechanical properties, and life-cycle assessment. J Clean Prod 223:662–679. https://doi.org/10.1016/j.jclepro.2019.03.077

Liu S, Zhu D, Li G et al (2018) Flexural response of basalt textile reinforced concrete with pre-tension and short fibers under low-velocity impact loads. Constr Build Mater 169:859–876. https://doi.org/10.1016/j.conbuildmat.2018.02.168

Lundberg SM, Lee SI (2017) A unified approach to interpreting model predictions. In: Advances in neural information processing systems, vol 30. Curran Associates, Inc.. https://proceedings.neurips.cc/paper_files/paper/2017/hash/8a20a8621978632d76c43dfd28b67767-Abstract.html

Malhotra VM (2010) Global warming, and role of supplementary cementing materials and superplasticisers in reducing greenhouse gas emissions from the manufacturing of Portland cement. Int J Struct Eng 1(2):5. https://doi.org/10.1504/IJSTRUCTE.2010.031480

Martínez-Ramón N, Calvo-Rodríguez F, Iribarren D et al (2024) Frameworks for the application of machine learning in life cycle assessment for process modeling. Clean Environ Syst 100221. https://doi.org/10.1016/j.cesys.2024.100221

Miller SA, Horvath A, Monteiro PJ (2016) Readily implementable techniques can cut annual CO_2 emissions from the production of concrete by over 20%. Environ Res Lett 11(7):074029. https://doi.org/10.1088/1748-9326/11/7/074029

Naseri H, Jahanbakhsh H, Hosseini P et al (2020) Designing sustainable concrete mixture by developing a new machine learning technique. J Clean Prod 258:120578. https://doi.org/10.1016/j.jclepro.2020.120578

Naseri H, Jahanbakhsh H, Khezri K et al (2022) Toward sustainability in optimizing the fly ash concrete mixture ingredients by introducing a new prediction algorithm. Environ Dev Sustain 24(2):2767–2803. https://doi.org/10.1007/s10668-021-01554-2

OECD (2019) Global material resources outlook to 2060: economic drivers and environmental consequences. OECD Publishing, Paris. https://doi.org/10.1787/9789264307452-en

Panesar DK, Seto KE, Churchill CJ (2017) Impact of the selection of functional unit on the life cycle assessment of green concrete. Int J Life Cycle Assess 22(12). https://doi.org/10.1007/s11367-017-1284-0

Pearce AR, Hastak M, Vanegas JA (1995) A decision support system for construction materials selection using sustainability as a criterion. In: Proceedings of the NCSBCS conference on building codes and standards. Citeseer

Qin F, Zhang Z, Yin Z et al (2020) Use of high strength, high ductility engineered cementitious composites (ECC) to enhance the flexural performance of reinforced concrete beams. J Build Eng 32:101746. https://doi.org/10.1016/j.jobe.2020.101746

Rajput A, Iqbal MA, Gupta N (2018) Ballistic performances of concrete targets subjected to long projectile impact. Thin-Walled Struct 126:171–181. https://doi.org/10.1016/j.tws.2017.01.021

Rapin J, Teytaud O (2018) Nevergrad - a gradient-free optimization platform. https://GitHub.com/FacebookResearch/Nevergrad

Reddy KP, Rao BCM, Yadav MJ et al (2021) Comparative studies on LC^3 based concrete with OPC and PPC based concretes. Mater Today: Proceedings 43:2368–2372. https://doi.org/10.1016/j.matpr.2021.01.833

Romeiko XX, Zhang X, Pang Y et al (2023) A review of machine learning applications in life cycle assessment studies. Sci Total Environ 168969. https://doi.org/10.1016/j.scitotenv.2023.168969

Schneider M, Romer M, Tschudin M et al (2011) Sustainable cement production—present and future. Cem Concr Res 41(7):642–650. https://doi.org/10.1016/j.cemconres.2011.03.019

Scope C, Guenther E, Mielecke T et al (2022) Life cycle assessment of carbon concrete composites: a circular economy path beyond climate mitigation? Acta polytechnica CTU proceedings. http://hdl.handle.net/10467/106320

Scope C, Guenther E, Schütz J et al (2020) Aiming for life cycle sustainability assessment of cement-based composites: a trend study for wall systems of carbon concrete. Civil Eng Des 2(5–6). https://doi.org/10.1002/cend.202000024

Scope C, Vogel M, Guenther E (2021) Greener, cheaper, or more sustainable: reviewing sustainability assessments of maintenance strategies of concrete structures. In: Sustainable production and consumption, vol 26. https://doi.org/10.1016/j.spc.2020.12.022

Scrivener K, Martirena F, Bishnoi S et al (2018) Calcined clay limestone cements (LC3). Cem Concr Res 114:49–56. https://doi.org/10.1016/j.cemconres.2017.08.017

Shahrokhishahraki M, Malekpour M, Mirvalad S et al (2024) Machine learning predictions for optimal cement content in sustainable concrete constructions. J Build Eng 82:108160. https://doi.org/10.1016/j.jobe.2023.108160

Sharif SA, Hammad A (2019) Developing surrogate ANN for selecting near-optimal building energy renovation methods considering energy consumption, LCC and LCA. J Build Eng 25:100790. https://doi.org/10.1016/j.jobe.2019.100790

Signorini C, Nobili A (2022) Durability of fibre-reinforced cementitious composites (FRCC) including recycled synthetic fibres and rubber aggregates. Appl Eng Sci 9:100077. https://doi.org/10.1016/j.apples.2021.100077

Signorini C, Bracklow F, Hering M et al (2023) Ballistic limit and damage assessment of hybrid fibre-reinforced cementitious thin composite plates under impact loading. J Build Eng 80:108037. https://doi.org/10.1016/j.jobe.2023.108037

Stoiber N, Hammerl M, Kromoser B (2021) Cradle-to-gate life cycle assessment of CFRP reinforcement for concrete structures: calculation basis and exemplary application. J Clean Prod 280:124300. https://doi.org/10.1016/j.jclepro.2020.124300

Sun C, Wang K, Liu Q et al (2023) Machine-learning-based comprehensive properties prediction and mixture design optimization of ultra-high-performance concrete. Sustainability 15(21):15338. https://doi.org/10.3390/su152115338

Tawfik A, Signorini C, Mechtcherine V (2023) Direct assessment of the shear behavior of strain-hardening cement-based composites under quasi-static and impact loading: influence of shear span and notch depth. Cem Concr Compos 140:105119. https://doi.org/10.1016/j.cemconcomp.2023.105119

Tushar Q, Bhuiyan MA, Zhang G et al (2022) Application of a harmonized life cycle assessment method for supplementary cementitious materials in structural concrete. Constr Build Mater 316:125850. https://doi.org/10.1016/j.conbuildmat.2021.125850

United Nations Environment Programme (2024) Global status report for buildings and construction: beyond foundations: mainstreaming sustainable solutions to cut emissions from the buildings sector. https://doi.org/10.59117/20.500.11822/45095

Van den Heede P, Mignon A, Habert G et al (2018) Cradle-to-gate life cycle assessment of self-healing engineered cementitious composite with in-house developed (semi-) synthetic superabsorbent polymers. Cem Concr Compos 94:166–180. https://doi.org/10.1016/j.cemconcomp.2018.08.017

Van Den Heede P, De Belie N (2012) Environmental impact and life cycle assessment (LCA) of traditional and "green" concretes: literature review and theoretical calculations. Cem Concr Compos 34(4). https://doi.org/10.1016/j.cemconcomp.2012.01.004

Williams Portal N, Lundgren K, Wallbaum H et al (2015) Sustainable potential of textile-reinforced concrete. J Mater Civ Eng 27(7):04014207. https://doi.org/10.1061/(ASCE)MT.1943-5533.0001160

Yoo DY, Banthia N, Kim SW et al (2015) Response of ultra-high-performance fiber-reinforced concrete beams with continuous steel reinforcement subjected to low-velocity impact loading. Compos Struct 126:233–245. https://doi.org/10.1016/j.compstruct.2015.02.058

Zea Escamilla E, Wallbaum H (2011) Environmental savings from the use of vegetable fibres as concrete reinforcement. In: 6th International structural engineering and construction conference, pp 1315–1320

Zhang J, Huang Y, Ma G et al (2021) Mixture optimization for environmental, economical and mechanical objectives in silica fume concrete: a novel frame-work based on machine learning and a new meta-heuristic algorithm. Resour Conserv Recycl 167:105395. https://doi.org/10.1016/j.resconrec.2021.105395

Zhang J, Huang Y, Aslani F et al (2020a) A hybrid intelligent system for designing optimal proportions of recycled aggregate concrete. J Clean Prod 273:122922. https://doi.org/10.1016/j.jclepro.2020.122922

Zhang J, Huang Y, Wang Y et al (2020b) Multi-objective optimization of concrete mixture proportions using machine learning and metaheuristic algorithms. Constr Build Mater 253:119208. https://doi.org/10.1016/j.conbuildmat.2020.119208

Zhang D, Jaworska B, Zhu H et al (2020c) Engineered cementitious composites (ECC) with limestone calcined clay cement (LC^3). Cem Concr Compos 114:103766. https://doi.org/10.1016/j.cemconcomp.2020.103766

Authors and Affiliations

Isabela de Paula Salgado[1,2] · Felix Conrad[3] · Cesare Signorini[2] · Edeltraud Günther[1,4] · Steffen Ihlenfeldt[3] · Viktor Mechtcherine[2]

✉ Cesare Signorini
cesare.signorini@tu-dresden.de

[1] Institute for Integrated Management of Material Fluxes and of Resources, UNU-Flores, Dresden 01067, Germany

[2] Institute of Construction Materials, TU Dresden, Dresden 01187, Germany

[3] Chair of Machine Tools Development and Adaptive Controls, TU Dresden, Dresden 01062, Germany

[4] Chair of Business Management, esp. Sustainability Management and Environmental Accounting, TU Dresden, Dresden 01062, Germany